Journal of Magnetic Resonance **152,** 168–178 (2001)
doi:10.1006/jmre.2001.2392, available online at http://www.idealibrary.com on IDEAL®

Low-Power *Wa*ter *S*uppression by *H*yperbolic Secant Pulses with *C*ontrolled *O*ffsets and *De*lays (WASHCODE)

Z. Starčuk, Jr.,*[,1] Z. Starčuk,* V. Mlynárik,† M. Roden,‡ J. Horký,* and E. Moser†·§

*Institute of Scientific Instruments, Academy of Sciences of the Czech Republic, 61264 Brno, Czech Republic; †NMR Group, Institute of Medical Physics, University of Vienna, Vienna, Austria; ‡Department of Internal Medicine III, University Hospital of Vienna, Austria; and §Department of Radiodiagnostics, University Hospital of Vienna, Austria

Received February 23, 2001; revised June 11, 2001; published online August 1, 2001

A class of chemical-shift-selective (CHESS) water suppression (WS) schemes is presented in which the characteristic frequency-domain excitation profiles of "adiabatic" full-passage (AFP) RF pulses are utilized for frequency-selective excitation of the water resonance. In the proposed WS schemes, dubbed WASHCODE, hyperbolic secant (HS) pulses were used as the AFP pulses. Besides the high immunity of WS efficiency toward B_1 inhomogeneity, these sequences also exhibit extraordinary insensitivity to the dispersion of the water T_1 relaxation times. The actual performance of the proposed WS schemes was achieved in particular by optimizing the frequency offsets of WS HS pulses and the time intervals between them. To reduce the RF power requirements of these WS sequences for *in vivo* applications, HS pulses with the minimum possible frequency bandwidths were employed, which also substantially reduced the adverse effects on the observed proton MR spectra. The proposed WS schemes were evaluated by simulations based on the Bloch equations. Several WS sequences which looked particularly promising were verified experimentally on the human brain on a 3 T MR scanner using very short echo-time STEAM for volume selection and a standard single-loop surface coil for both signal transmission and reception. Routinely, water-suppression factors ranging from 2000 to 4000 were achieved *in vivo* without additional adjustment of parameters for individual subjects and without violating legal safety limits. © 2001 Academic Press

Key Words: **low-power water suppression; B_1 insensitive; T_1 insensitive; adiabatic full-passage pulses; hyperbolic secant pulses.**

INTRODUCTION

Despite the ability of modern MR scanners to adequately digitize metabolite signals at concentrations even lower than 1 mM in the presence of large amounts of tissue water (*1*), highly efficient water suppression (WS) is often still required in human *in vivo* proton MR spectroscopy. WS helps to avoid spectral distortions arising from imperfectly suppressed false coherence pathways, imperfect volume selection, or acoustic resonances related to strong and fast-switched magnetic field gradients.

Water suppression techniques for *in vivo* proton MRS are based on exploiting a suitable physical parameter distinguishing the protons of water from those of the observed metabolites. In short echo-time *in vivo* proton MRS, water suppression is almost exclusively accomplished by chemical-shift-selective (CHESS) techniques, based on the difference between the chemical shifts of water and of metabolite protons (*2–15*). With CHESS techniques, the water resonance is saturated, as a rule, by repeating episodes of water magnetization excitation and subsequent dephasing by strong magnetic field gradient pulses. Water suppression efficiency achieved with the CHESS WS techniques proposed so far is always affected by inhomogeneities of the exciting B_1 field and by the inhomogeneous T_1 relaxation of water. Therefore, the current developments of CHESS WS sequences for *in vivo* applications are driven by the desire to make WS efficiency insensitive to both these parameters. In addition, there are other important properties to be considered when designing a WS technique, such as RF power deposition (SAR), tolerance toward B_0 inhomogeneity, adverse effects on metabolite resonances occurring close to the water resonance, compatibility with very short echo-time acquisition, and possibility of accommodating outer volume suppression or other magnetization preparation, as well as time demands for implementation and experimental adjustments *in vivo*.

In most CHESS-type WS techniques, water excitation is accomplished by amplitude-modulated RF pulses whose carrier is set exactly on the water resonance (*2–13*). Recently, de Graaf and Nicolay proposed a different WS technique, called SWAMP, in which water excitation is carried out by the transition zones of frequency-domain excitation profiles of adiabatic full passage (AFP) RF pulses (*14*). The carrier frequency of these AFP RF pulses is offset from the water resonance by about one-half of their total frequency sweep width. Due to the properties of AFP pulses, SWAMP exhibits strong immunity toward the B_1 field inhomogeneity. However, the original SWAMP sequence has two major drawbacks: its RF power requirements are too high for whole-body application, and its WS efficiency is substantially

[1] To whom correspondence should be addressed at Institute of Scientific Instruments, Academy of Sciences of the Czech Republic, Královopolská 147, 61264 Brno, Czech Republic. Fax: +420-5-4151 4402. E-mail: starcuk@isibrno.cz.

1090-7807/01 $35.00
Copyright © 2001 by Academic Press
All rights of reproduction in any form reserved.

compromised by T_1 relaxation during the AFP pulses and the delays between them. The former problem might be alleviated by narrowing the excitation bandwidth (and sacrificing part of the spectral width), but this would even aggravate the second problem. The benefits of shortening the interpulse delays to values as low as 1 ms, as proposed by the authors, are questionable: it does not eliminate T_1 relaxation during AFP pulses and it reduces the achievable efficiency of crushing unwanted transverse magnetizations by gradients due to gradient strength or slew-rate limitations and the increased liability to eddy currents. As a result, in whole-body MR systems, the original SWAMP does not assure the desired high WS efficiency within legal safety limits.

Recently, a modification of the SWAMP sequence has been proposed (*15*) which demonstrates that the performance of these sequences can be substantially improved by simultaneous optimization of the RF pulse offsets and the delays between them. Such sequences can be made insensitive to the heterogeneity of the B_1 field and efficient in a wide range of T_1 relaxation times of water protons. Because of the long delays (typically tens of milliseconds), outer volume suppression (OVS) modules may be accommodated close to the localizing excitation. Furthermore, these sequences exhibit improved frequency-domain excitation profiles of the water suppression region, and are very robust and flexible. Despite the higher number of parameters, their implementation and application are very easy and fast, which is vitally important for *in vivo* experiments.

This paper deals with the theoretical background and further developments of the latter type of the CHESS WS schemes. The main attention is focused on minimizing the RF power requirements of these WS sequences without introducing adverse effects on the spectral range of interest. In the present paper we demonstrate that RF power deposition generated by AFP pulse sequences may become comparable with that of other multipulse CHESS WS schemes if suitable AFP pulses of the minimum applicable bandwidth are used. The properties of the designed WS schemes were analyzed in detail by computer simulation based on a numerical solution of the Bloch equations, taking into account the basic parameters characterizing the subject (i.e., T_1, T_2) and the complete excitation sequence comprising STEAM localization (*16*) and WS in the preparatory period as well as in the middle period *TM* of STEAM. Power deposition of the newly proposed WS sequences is compared with that of the most commonly employed WS techniques. Experimental verification was carried out in the human brain on a 3 T MR scanner.

THEORY

Water-Excitation RF Pulses

AFP RF pulses have been found attractive for various applications due to their ability to produce defined spin manipulation with little sensitivity toward B_1-field inhomogeneity. At RF power levels exceeding a certain threshold level, the frequency-domain excitation profiles of these pulses are practically independent of B_1. In either transition zone around the excitation bandwidth of a spin-inversion AFP pulse there exists a frequency offset for which the pulse performs a 90° excitation. Together with a suitable RF pulse frequency offset this provides a convenient way for B_1-insensitive excitation of water protons (*14*). In CHESS WS techniques, a flat region of suppression around the water resonance and a minimal effect on other signals are desirable. The final frequency-domain excitation profile results from multiplicative shaping of the initial magnetization and new inseparable T_1-relaxation admixtures by the appropriate coherence-transfer profiles of the RF pulses applied. The profiles forming the suppression region, as well as the miminum power required, depend on the type of amplitude and frequency modulation of the AFP pulse. A very sharp transition zone resulting in a narrow suppression bandwidth can be achieved with Lorentzian amplitude modulation, however, at the cost of higher peak RF power and some profile distortions at low RF power levels (*14*). On the other hand, the well-known hyperbolic secant (HS) pulses (*17*) appear very convenient for the construction of WS schemes of the above-mentioned type.

A basic HS pulse with frequency sweep from $-F$ to $+F$ [Hz] during a time interval $-T/2 \le t \le T/2$ is described by amplitude modulation $\gamma B_1(t) = b \text{ sech } (t/\tau)$ [Hz] and frequency offset $\nu(t) = F \tanh(t/\tau)$ [Hz]. The time-scale parameter τ is related to the maximum sweep rate at the pulse center, $(\mathrm{d}\nu/\mathrm{d}t)(0) = F/\tau$. To describe the pulse shape and the particular type of excitation in a time-scale-independent way, it is convenient to define the relative B_1 amplitude $q = b/|F|$, the time-extension factor $\lambda = T/\tau$, and the sweep factor $n = F\tau$. For the actual implementation the pulse shape is fully determined by parameters n and λ, and the excitation bandwidth Δ is basically identical to the sweep range $2F$. The exact value of parameter λ, defining the cutoff level $\varepsilon = B_1(T/2)/B_1(0)$, is not critical. As a suitable compromise between the pulse duration and the truncation artifacts, $\lambda = 10.0$ ($\varepsilon \approx 1.3\%$) is further assumed for all pulses. With the value of λ fixed, notation HS n is sufficient to identify a specific HS pulse type. For the elimination of the endpoint discontinuity, amplitude reduction to $\gamma B_1'(t) = \gamma B_1(t) - \gamma B_1(T/2)$ was proposed (*14*); such pulses will be denoted as HS n'.

The general HS pulse performance, manifested by the shape of excitation profiles, is closely related to parameter n. While the typical values $|n|$ used for adiabatic inversion pulses are 0.5 to 1.0, specific goals may be better achieved with other values ($0.2 < |n| < 2.0$). Computer simulation, whose substantial results are summarized in Table 1A, reveals several facts: (1) For a given excitation bandwidth, HS pulses with higher values of n are longer, deposit more RF energy, and their frequency-domain excitation profiles are closer to rectangular due to improved adiabaticity. (2) With any HS pulse, sufficient transition-region stability toward B_1 (e.g., such that the full-excitation offsets do not change by more than $\delta_\nu \approx 3$ Hz with a 30-ms pulse, i.e., $\delta_\nu \tau < 0.01$) is achieved already with B_1 values above B_{1t} at $\sim 90\%$ of the spin-inversion threshold value B_{1i}. (3) If $|n| \ge 0.3$, usage of HS pulses with a higher sweep factor n only negligibly improves the transition region stability, whose main

TABLE 1
Basic Power- and Bandwidth-Related Properties of the RF Pulses Referred to in This Paper (Relaxation Effects Neglected)

A. HS pulses

Pulse[a]	$q\mathrm{i}^b$	$q\mathrm{i}^b$	$q\mathrm{e}^b$	$T\,\Xi^c$	$T\,\Delta^c$	Ξ/Δ^c
HS ±0.2	1.30[d]	1.07	0.585	1.36[d]	4.00	0.340[d]
HS ±0.3	1.02	0.880	0.457	1.87	6.00	0.312
HS ±0.5	0.870	0.730	0.357	3.78	10.0	0.378
HS ±1.0	0.672	0.536	0.260	9.03	20.0	0.452
HS ±2.0	0.504	0.413	0.180	20.3	40.0	0.508
HS ±5.0	0.325	0.295	0.125	52.8	100	0.528

B. Amplitude-modulated pulses

Pulse[a]	$T\,\Xi^c$	$T\,\Delta^c$	$\Xi\Delta^c$
90° SINC3	0.317	5.16	0.0614
90° GAUSS	0.112	1.64	0.0683
90° P10	0.372	5.24	0.0710
180° M8	2.65	5.66	0.468
90° RECT	0.0625	0.86[e]	0.0727[e]

[a] Pulses HS described in text; P10 and M8 are our optimized asymmetric pulses used in STEAM and VAPOR (*9*), other pulses standard (SINC3 = 3-lobe sinc, GAUSS = gaussian, RECT = rectangular).

[b] Relative B_1 levels corresponding to the thresholds of adiabatic inversion ($q_\mathrm{i} = \gamma B_{1\mathrm{i}}/F$, 99% inversion efficiency at zero offset), transition-zone stability ($q_\mathrm{t} = \gamma B_{1\mathrm{t}}/F$, definition in text), and to 90° excitation ($q_\mathrm{e} = \gamma B_{1\mathrm{e}}/F$, at zero offset).

[c] Pulse length T. Excitation bandwidth Δ at 50% between the nonexcited and fully excited M_z level. Energy factor $\Xi = \int_0^T (\gamma B_1(\mathbf{r}_0, t))^2\,\mathrm{d}t$, where $\mathbf{r}_0$ is the point for which the power level is set. Specifically for HS pulses, B_1 level corresponding to q_i used; for levels q_t, q_e the Ξ scaling factors are $(q_\mathrm{t}/q_\mathrm{i})^2$ and $(q_\mathrm{e}/q_\mathrm{i})^2$, respectively.

[d] $M_z < -0.99\,M_0$ valid only in intervals of B_1; this value valid for the center of the first such interval.

[e] Highly nonrectangular excitation profile.

indicators are the frequency position ν^* of the $M_z(\nu)$ zero crossing (Fig. 1) and the slope $\mathrm{d}M_z(\nu)/\mathrm{d}\nu$ at this point. (4) Application of the modified pulses HS n' instead of pulses HS n improves the transition-zone stability for slower swept pulses (such as $|n| \geq 1$), but it has no practical effect with faster swept pulses ($|n| \leq 0.3$). (5) For a fixed pulse duration T (or rather τ) the transition zone bandwidth Δ_t (understood as the frequency range in which $|M_z| < 0.95\,M_0$ after the excitation of fully relaxed magnetization M_0 by an AFP pulse with its power set above the inversion threshold $B_{1\mathrm{i}}$) is practically independent of the sweep factor n and can be estimated as $\Delta_\mathrm{t} \approx 3.8/T$.

Based on this knowledge, it may be concluded that application of HS pulses with $|n| > 0.3$ in the WS schemes considered is not advantageous unless high-quality inversion is required for another reason.

With the expected pulse durations of 30–50 ms, neither T_1 nor T_2 relaxation can be neglected. Simulations show that T_2 relaxation has a negligible effect in the vicinity of the full-excitation offsets. T_1 relaxation during the pulse, however, significantly affects the transition zone and cannot be neglected in the design nor in the implementation of WS sequences. The transition region around offset $-F$ is excited earlier and is more affected by relaxation. Therefore, pulses with opposite frequency-sweep directions are not interchangeable in T_1-relaxation-optimized sequences. In the proposed WS sequences, the frequency sweep will always be oriented toward the transition zone used for water excitation (i.e., $F < 0$ for downfield-offset pulses).

To reduce the energy deposited by the HS pulses, it is desirable to use the lowest excitation bandwidths possible. With the transition-zone excitation and the focus on the upfield part of the spectrum, corruption of a part of the spectral range on the downfield side of the water resonance and, thus, collection of one-sided spectra only are acceptable. The selection of pulse parameters is driven by several requirements. The width of the transition region Δ_t should not exceed ~1 ppm so that metabolites in a window of up to 4.3 ppm can be detected. The above-mentioned simulation results indicate that a pulse duration $T > 29.7\,\mathrm{ms} \times (3\,\mathrm{T}/B_0)$ is required. On the other hand, the bandwidth Δ_t should not be much narrower to cope well with B_0 inhomogeneity. With regard to T_2-relaxation times it seems reasonable to keep the pulse length T shorter than ~60 ms. Suitable pulses are those with $|n| = 0.2$ or, for better stability, $|n| = 0.3$ with durations $T \geq 30\,\mathrm{ms} \times (3\,\mathrm{T}/B_0)$. At 3 Tesla, downfield-offset 30- to 40-ms pulses HS −0.2 or 30- to 50-ms pulses HS −0.3′ were found convenient.

For a comparison, full spectral bandwidth inversion (used in SWAMP and applicable also with WASHCODE) requires an excitation bandwidth of ≥5 ppm, i.e. $T \approx 2|n|\lambda/\Delta < 1.3\,\mathrm{ms} \times |n| \times (3\,\mathrm{T}/B_0)$. To meet both bandwidth requirements,

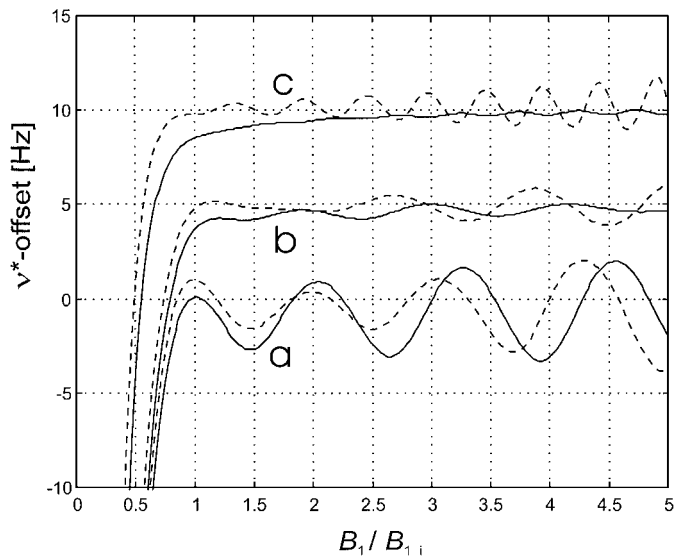

FIG. 1. B_1 sensitivity of the frequency position (ν^*) of 90° excitation by hyperbolic secant (HS) pulses. Simulation for pulses (a) 30-ms HS 0.2 (frequency sweep range $2F = 133$ Hz), (b) 40-ms HS 0.3 ($2F = 150$ Hz), (c) 30-ms HS 1.0 ($2F = 667$ Hz), with (solid) or without (dashed) cutoff level nulling (*14*). No relaxation considered. B_1 normalized to the respective adiabatic inversion thresholds $B_{1\mathrm{i}}$. For graph clarity, offsets $\nu^* - F$ are shown, further shifted by (a) 0 Hz, (b) 5 Hz, and (c) 10 Hz.

slow-sweep HS pulses ($|n| \geq 1.0$) must be used, e.g., HS $\pm 1.0'$ pulses with $T = 30\ \text{ms} \times (3\,\text{T}/B_0)$.

Pulse Sequence

The class of WS sequences, for which we propose the acronym WASHCODE (*Wa*ter *S*uppression by *H*yperbolic Secant Pulses with *C*ontrolled *O*ffsets and *De*lays), is based on water excitation by the transition zones of the excitation profiles of frequency-offset HS pulses. By exploiting the upfield zones of downfield-offset pulses, upfield resonances are undisturbed by the water excitation. The sequences consist of two modules: (1) A presaturation sequence with m (2 to 4) HS pulses with optimized RF pulse offsets and timing, with delays containing dephasing B_0 field gradients and, optionally, RF pulses and gradients for OVS. (2) A localization module, selecting the volume of interest (VOI) and optionally including additional WS. STEAM, is particularly useful because its *TM* interval is capable of accommodating large crusher gradients and optionally also WS. This WS may considerably improve the overall WS efficiency because of its T_1 insensitivity, resulting from the separability of the coherence pathway leading to the stimulated echo from that of T_1-restored magnetization. As increasing the length of *TM* leads to a loss of metabolite signal due to T_1-relaxation, we suggest to use only one WS pulse in the *TM* period.

The general structure of such pulse sequences is

[WS{+OVS}]–[Localization{+WS}]–Acquisition/Recovery,

or, in more details for STEAM localization (Fig. 2),

$$[\text{W}_k - d_k]_{k=m\cdots 1}\text{–(P}_1\text{)–}t_{\text{e1}}\text{–(P}_2\text{)–}t_{\text{m1}}\text{–\{(W}_0\text{)\}–}t_{\text{m2}}\text{–(P}_3\text{)–}t_{\text{e2}}\text{–Acq./Recovery,}$$

where braces indicate optional elements, symbols P_i ($i = 1\cdots 3$) represent the three-slice-selection pulses of STEAM, W_k($k = 0\cdots m$) denote the water excitation HS pulses, and d_k and t_α stand for the time intervals between RF pulses (measured to the RF pulse focus point where indicated by a parenthesis at the adjacent pulse symbol so that pulse shape dependence might be avoided). Interval d_1 can, therefore, be expressed independently of the type of pulse P_1. Pulses W_k($k \geq 1$), selected as described above, are identical except for their frequency offsets ν_k. These offsets and delays d_k must be optimized simultaneously to provide suitable frequency domain excitation profiles insensitive to T_1. The B_1 insensitivity results from the properties of excitation by HS pulses. The optional pulse W_0 inserted in *TM* may be identical with the presaturation pulses, with its full-excitation offset set exactly on the prevalent water resonance frequency.

Our optimization of HS pulse offsets and timing was based on computer simulation. An evolutionary trial-and-error process was found useful in which new pulses were added with optimized parameters before previously optimized sequence fragments. However, to customize the sequence parameters for specific sets of priorities (e.g., suppression factor, B_0 inhomogeneity, minimum or maximum delays), numeric optimization might be preferable. Our minimized objective function was constructed as a sum of WS-imperfection penalties for $T_1 = 0.7$, 1.1, and 1.5 s. Each of them was based on the absolute values of M_z at the end of interval d_1 inside a limited frequency offset interval (20 Hz) around the water resonance, to which a suitable weighting was applied. To confine any delay in certain limits, out-of-bounds values were severely penalized by a high-order polynomial function. With such a task definition, a standard minimization algorithm implemented in Matlab (The Math Works, Inc., Natick, MA) could be used. Equal delays of 20 ms

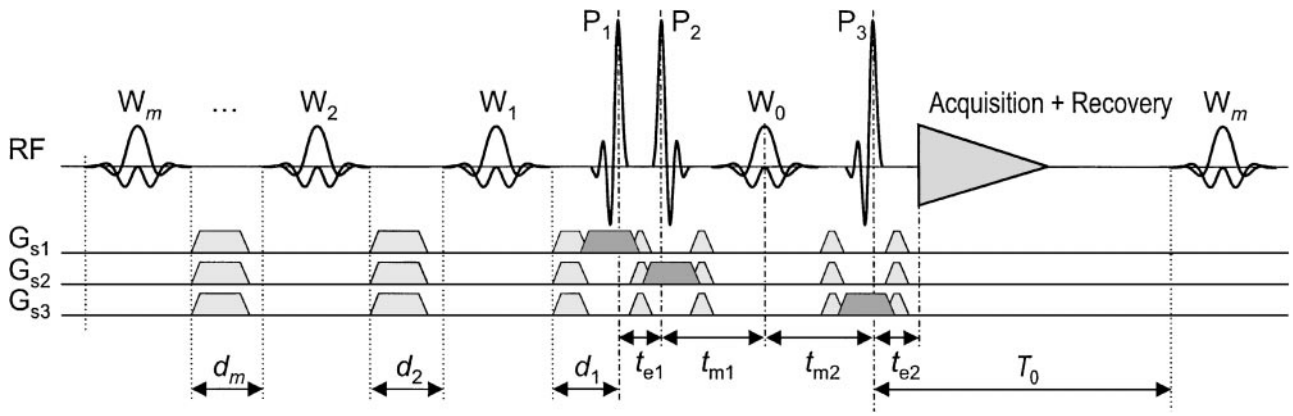

FIG. 2. Structure of WASHCODE pulse sequences with STEAM localization. Transition zones of the frequency-domain excitation profiles of hyperbolic secant (HS) pulses are used for water excitation. The frequency offsets of the otherwise identical HS pulses $\text{W}_m, \ldots, \text{W}_1$($m = 2\cdots 4$) and of the interpulse delays $d_m, \ldots, d_1$ are chosen such as to provide good frequency-domain profiles in the suppression region with minimum T_1 sensitivity. Delays d_k provide enough time for crusher gradients and for the incorporation of outer volume suppression. T_1 insensitivity may be improved by an additional pulse W_0 inserted in the $TM = t_{\text{m1}} + t_{\text{m2}}$ period of STEAM with slice selection pulses P_1, P_2, and P_3. For minimal outer-volume contamination and/or short echo time $TE = 2t_{\text{e1}} = 2t_{\text{e2}}$, optimized asymmetric pulses are recommended for slice selection. HS pulses are followed by dephasing gradient pulses such as to avoid spurious echo formation. Timing and amplitudes not to scale. Details in text.

TABLE 2
WASHCODE Sequence Parameters (Examples)

WS pulse	T [ms]	F [Hz]	m	Offsets $\nu_m, \ldots, \nu_1, (\nu_0)^a$ [Hz]	Delays $d_m, \ldots, d_1$ [ms]
HS $-0.3'$	30	-100.0	1	94.2, (98.2)	77.7
			2	103.6, 89.5	36.2, 16.4
			3	108.4, 99.1, 85.0	30.8, 34.2, 9.3
			4	101.5, 106.2, 92.6, 73.9	22.8, 35.8, 19.2, 5.6
	40	-75.0	1	72.0, (73.6)	36.5
			2	77.2, 66.1	51.6, 15.3
			3	82.4, 72.8, 62.5	58.2, 42.6, 9.0
			4	76.9, 80.7, 69.9, 55.6	30.0, 44.1, 19.8, 9.6
	50	-60.0	1	50.0, (58.9)	233.2
			2	63.3, 52.1	25.6, 20.7
			3	65.9, 59.5, 48.8	26.2, 24.1, 9.4
			4	61.5, 63.9, 56.8, 41.3	25.4, 24.9, 19.0, 18.9
HS $-1.0'$	30	-333.3	1	322.0, (331.5)	148.7
			2	333.3, 319.9	164.2, 32.0
			3	343.1, 332.2, 317.5	21.5, 32.2, 9.3
			4	340.4, 334.9, 324.9, 303.3	21.7, 40.7, 18.8, 11.7

[a] All pulse offsets relative to the water resonance frequency in the VOI center. Offsets ν_0 shown in parentheses for $m = 1$ are valid for any m.

and offsets of half the sweep range F were used as the starting points. Although no attempt was made to find global minima, sufficiently good solutions have been found in this way. Some suitable sets of parameters, calculated for the recovery time of 2.5 s, are listed in Table 2. All offsets in this table are relative to the water resonance frequency.

METHODS

Simulation

Computer simulation based on numerical solution of the Bloch equations including both T_1 and T_2 relaxation was applied as the first stage of verification. The whole sequences including coherence pathway separation were evaluated. The slice-selection pulses of STEAM were modeled by 1 μs hard pulses in order to isolate the effects of water suppression from the off-resonance effects of slice selection (i.e., slice profile and chemical-shift displacement), which are unrelated to water suppression and depend on the shaped RF pulses and gradients applied.

Experiment

Several WASHCODE sequences were experimentally verified on a 3 T Medspec-DBX MR scanner (Bruker Medical Inc., Ettlingen, Germany), using a 55-cm i.d. gradient coil system (Bruker BGA 55) and a standard single-loop 10-cm-diameter transmit/receive surface coil. A modified STEAM sequence (Fig. 2) with 2.15-ms localization pulses with bandwidths of 2700 Hz (optimized asymmetric pulses minimizing out-of-slice excitation (*9*, *18*), or standard 3-lobe sinc pulses) was used for the acquisition of localized MR spectra from a $2 \times 2 \times 2$ cm^3 VOI centered about 3 cm below the skull, i.e., 2 cm above the coil plane, in the occipital lobe of a healthy volunteer ($TE =$ 7 ms, $TM =$ 50 ms, $TR =$ 2500 ms). Based on theoretical computations for such a configuration, the ratio between the maximum and the minimum B_1 value inside the VOI was approximately 1.5. The 30-ms WS pulses HS -0.2 were frequency offset for downfield excitation. Before the actual measurement, manual shimming for the VOI was performed and power levels were adjusted. First, with WS switched off, the power of STEAM pulses was adjusted for a maximum signal of water. Then the power level of presaturation HS pulses was increased nearly to the inversion threshold value to achieve stable water suppression. Finally, the power of pulse W_0 was set to a similar value. The power levels of all pulses are set based on the pulse performance in the VOI and, therefore, their ratios can be precalculated.

In all experiments, 4×4-step-phase cycling of pulses P_3 and P_2 was used, embedded in a CYCLOPS supercycle (*19*). For excitation, coronal RF coil orientation was used. Slices were selected in the order coronal (slice $\perp y$), sagittal (x), axial (z), with B_0 gradients of 1350 Hz/cm. The dephasing effects of gradients $\mathbf{g}(t)$ in intervals d_3, d_2, d_1, t_{e1}, t_{m1}, t_{m2}, and t_{e2}, evaluated by the corresponding k-space offsets (at coherence level $+1$) $\Delta\mathbf{k} = (\Delta k_x, \Delta k_y, \Delta k_z) = \int \gamma \mathbf{g}(t)\,dt$, were (100, 0, 0), (0, 0, 100), (0, 100, 0), (25, 0, 10), (33, 0, 0), (0, 0, 150), and (25, 0, 10) cm^{-1}, respectively.

^{1}H MR spectra of human brain tissue were obtained from the same VOI with a $3 + 1$-pulse WASHCODE sequence with different HS-pulse power levels ranging from B_{1t} to $4B_{1t}$. Signals were accumulated in 256 scans, and truncated to 0.2 s sampled by 500 complex points starting at the echo center. Lorentzian line broadening of 1.3 Hz and zero filling to 8 K points were applied before the Fourier transform, and only 0th order phase correction was used.

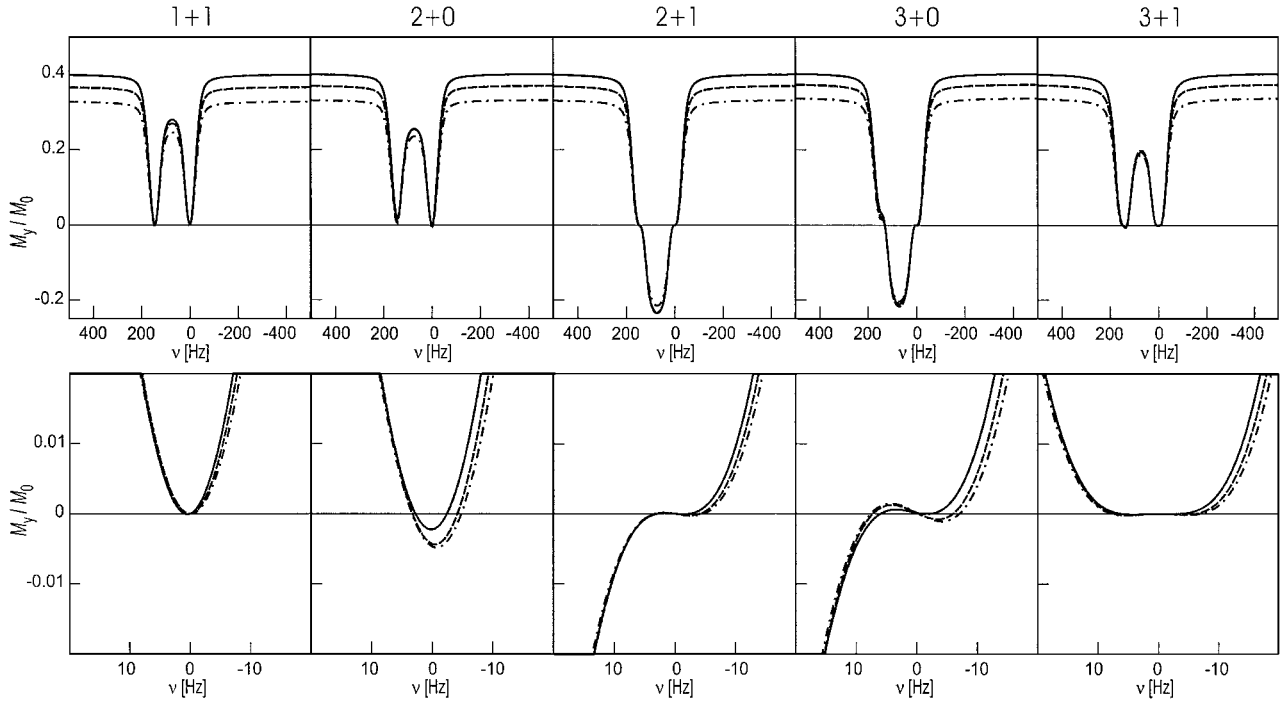

FIG. 3. Frequency-domain excitation profiles $M_y(\nu)$ of the stimulated echo in WASHCODE-STEAM sequences with $m = 1$, 2, and 3 presaturation pulses, without ($m + 0$-pulse WASHCODE) or with ($m + 1$-pulse WASHCODE) the WS pulse W_0 in *TM*. The dependences are plotted for water $T_1 = 0.7$ s (solid), 1.1 s (dashed), and 1.5 s (dash-dot), $T_2 = 0.1$ s, and B_1 set to the adiabatic inversion threshold B_{1i}, which ensures efficient WS in a VOI with $B_{1\,\max}/B_{1\,\min} < 1.3$. In all simulations $TE = 10$ ms, $TM = 50$ ms, and the slice-selection flip angle is 90°.

RESULTS

Simulation

Figure 3 demonstrates the role of the number of WS pulses. It proves that by employing more HS pulses generally more reliable WS is achieved, and that the application of pulse W_0 in *TM* is superior to adding an extra presaturation pulse. It further indicates that with the extra HS pulse in period *TM*, WS-factors of >10000 can be achieved under closely controlled conditions and >1000 on a routine basis.

The insensitivity of WS efficiency to simultaneous T_1 and B_1 variation is demonstrated in Fig. 4. Comparison between graphs (a) and (b) illustrates the fact that in very inhomogeneous B_1 fields the degradation of WS efficiency in low-B_1 areas can be overcome by increasing the power of the HS pulses with respect to the slice-selection pulses.

The intensities of the spectral lines of interest occurring close to the water resonance frequency may be affected by the WS to some extent. Simulations confirm that there is no observable offset-dependent bias due to T_1 relaxation because of the very limited excitation of the upfield region; only the standard TR/T_1-dependent saturation recovery can be observed. The offset-dependent partial saturation is determined mainly by the ratio between T_2 and the pulse length T, and by the magnitude of the B_1 field applied. This effect is illustrated in Fig. 5, simulating the excitation of metabolites by $3 + 1$-pulse WASHCODE sequences adapted for different B_0 fields and applying various B_1 power levels. Obviously, with increased power levels and/or with the larger durations of HS pulses required at lower B_0 fields the impact increases. In reality, the effect in lower fields will be less pronounced than shown because of the slightly higher T_2 values (*20*).

A comprehensive theoretical comparison of WASHCODE a SWAMP is hardly possible because of the system and sample dependency of the spectral distortions due to insufficient WS. For instance, an elevated intensity of wrong-pathway signals not localized within the VOI will require the application of high gradients, which may lead to distortions by eddy currents and mechanical vibrations. Nevertheless, a partial comparison may be based on the evaluation of the main-pathway water magnetization. Figure 6 provides the comparison of a WASHCODE sequence with two SWAMP-like sequences without optimized frequency offsets and delays. The simulations supposed either presaturation followed by STEAM localization with an additional WS pulse in period *TM*, or presaturation without such additional WS and with any type of localization (STEAM or PRESS). The comparison of the two types of application indicates how much of the resulting WS efficiency is derived from the WS in *TM*. The presaturation efficiency was found to be severely compromised in SWAMP-like sequences.

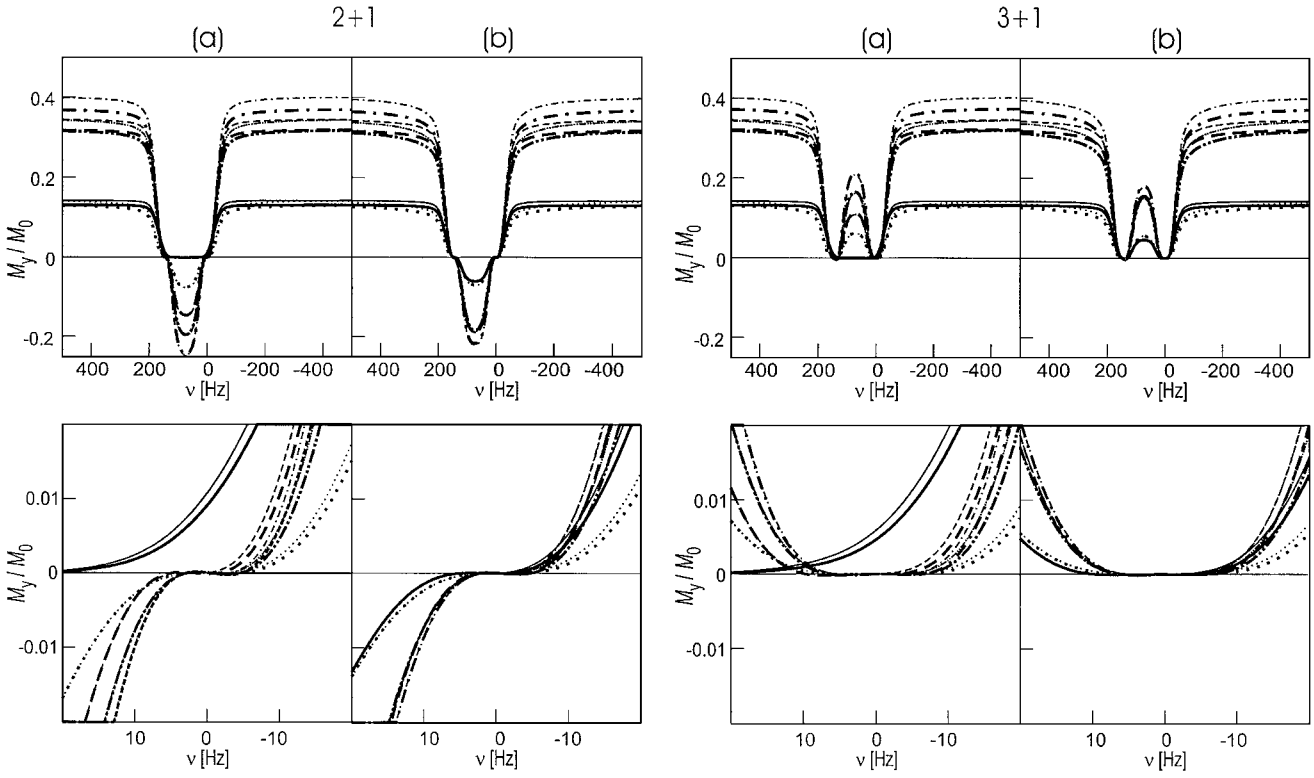

FIG. 4. Frequency-domain excitation profiles $M_y(\nu)$ of the stimulated echo in 2 + 1- and 3 + 1-pulse WASHCODE-STEAM sequences with the 40-ms HS $-0.3'$ pulse power level set to (a) 1.08 B_{1i} or (b) 1.73 B_{1i} at the point where the STEAM pulses produce a 90° flip angle, presumably the VOI center. These levels are chosen such as to ensure efficient WS in the VOI within a B_1 inhomogeneity range $B_{1\,max}/B_{1\,min}$ of 1.5 and 3, respectively. The excitation profiles are plotted for local B_1 equal to the 0.5 (—), 0.8 (– – –), 1.0 (– •), 1.2 (– • •), and 1.5 (• • •) times the nominal B_1 value valid in the VOI center, for $T_1 = 1.1$ s (thin) and 0.7 s (thick). The zoomed bottom graphs show details of the water-suppression region from the graphs above and document the robustness of WS efficiency. The dependence of M_y on B_1 in the nonsuppressed regions is mainly due to the slice-selection sensitivity to B_1.

Experiment

Typical ^{1}H MR spectra of human brain tissue are shown in Fig. 7. The water suppression factors can be estimated as ∼2600–4400. These values are lower than predicted theoretically, which can be explained by the B_1 and B_0 inhomogeneities inside the VOI. Fine adjustment of delay d_1 might improve the efficiency. Even with the highest B_1 level, the measured SAR was below the legal safety limits.

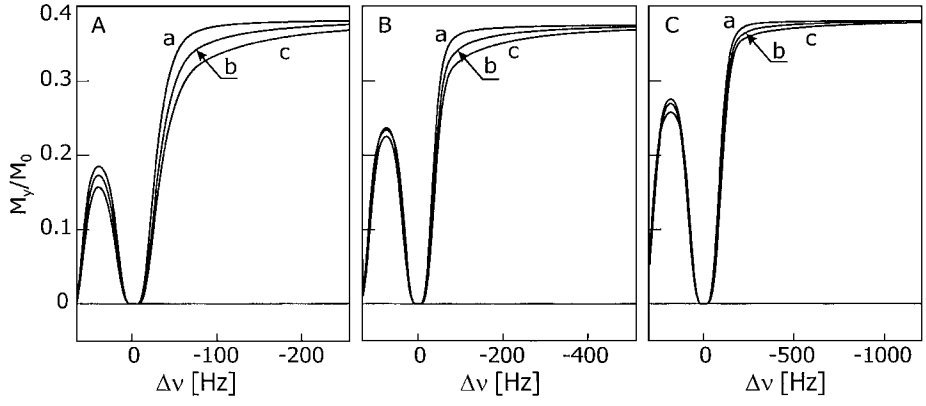

FIG. 5. Simulation of the saturation effect on metabolites. Frequency-domain excitation profiles $M_y(\nu)$ of the stimulated echo in the 3 + 1-pulse WASHCODE-STEAM sequence adapted for (A) 1.5 T (80-ms HS pulses), (B) 3 T (40-ms pulses), and (C) 7 T (16-ms pulses). Frequency range −4 to 1 ppm from the water resonance shown. Calculated for $T_1 = 1.3$ s and $T_2 = 0.2$ s, for HS pulse B_1 levels set to (a) 1.0 B_{1i}, (b) 2.0 B_{1i}, and (c) 3.0 B_{1i}. With the relaxation delay of 2 s, the full STE amplitude would be 0.39 M_0.

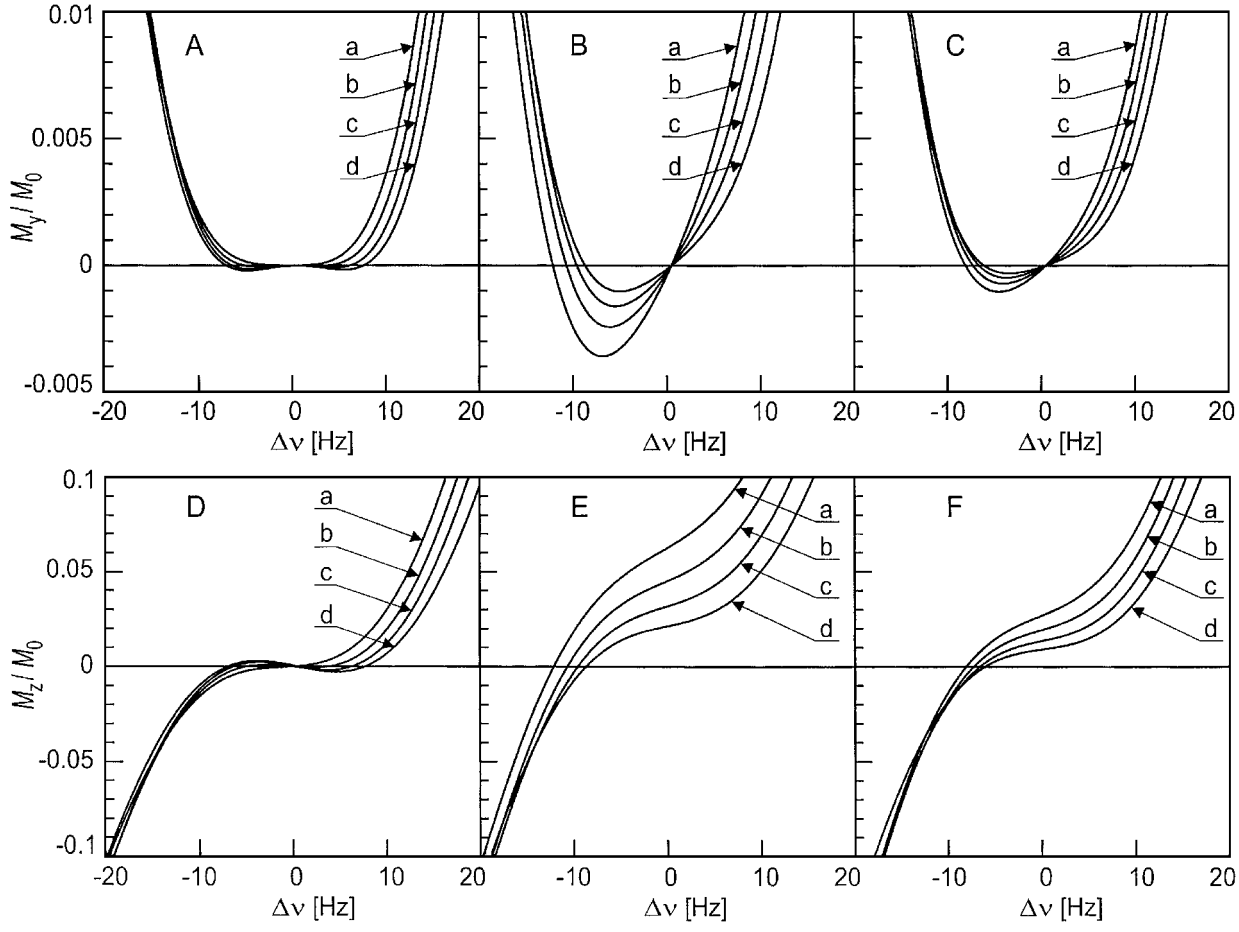

FIG. 6. Simulation of the WS efficiency in a 3-pulse WASHCODE sequence (A, D) and in 3-pulse SWAMP-like sequences with constant offsets and interpulse delays of 20 ms (B, E) and 1 ms (C, F). For SAR compliance, 40-ms HS $-0.3'$ pulses were used in all sequences. Graphs A, B, and C show the excitation profiles $M_y(\nu)$ after STEAM localization including one WS pulse in *TM* period (i.e., full signal is 0.5 M_0). Graphs D, E, and F show $M_z(\nu)$ at the end of presaturation and, therefore, describe the final magnetization M_y after localization with no additional WS (such as PRESS or STEAM with no WS in *TM*). The lines correspond to water proton T_1 of (a) 0.5 s, (b) 0.7 s, (c) 1.0 s, and (d) 1.5 s. $T_2 = 0.1$ s and $T_0 = 2$ s were assumed in all cases.

For comparison, spectra acquired in a similar manner, but with insufficient HS-pulse power ($0.7B_{1t}$), were found not only to have higher water/NAA ratios (∼5.5), but were also corrupted by modulation satellites disposed at ±170 Hz and ±940 Hz around the water resonance, with intensities of about 5% of the residual water line intensity.

DISCUSSION

WS sequences of the WASHCODE class, which belongs to the family of multipulse CHESS WS schemes, pursue several goals: efficient and robust water suppression, low side effects on other resonances, and low-power deposition.

Analogously to the recently proposed SWAMP technique, their insensitivity to B_1 field inhomogeneity is based on water excitation by the frequency-domain transition zones of AFP RF pulses. However, in contrast to SWAMP, WASHCODE sequences exhibit several advantages, such as considerable reduction of RF power requirements, high immunity of WS efficiency to the dispersion of the water T_1 relaxation time, and better adaptability to specific requirements. Reduction of the RF power deposition, which is a very important consideration in human studies, especially at high magnetic fields, was achieved by applying only a small number (i.e., 1 to 4) of fast-sweep AFP pulses, such as HS 0.3 pulses, with reduced frequency bandwidths ($2|F| = 150$ Hz at 3 T field, i.e., ∼1.2 ppm) and B_1 levels as low as possible ($b/|F| \geq 0.9$ inside the VOI). The use of narrowband HS pulses resulted in a reduction of the adverse effects on the spectrum of interest, located outside the WS excitation band. The immunity of the WS efficiency to the dispersion of the water T_1 relaxation time was achieved by simultaneous optimization of the frequency offsets of the WS RF pulses and the relatively long time delays between them. It was confirmed experimentally that the inclusion of one WS HS pulse in the *TM* period of STEAM considerably improves the WS efficiency, which is extremely valuable for short echo-time experiments. All HS pulses are identical except for their frequency offsets, which makes the WASHCODE

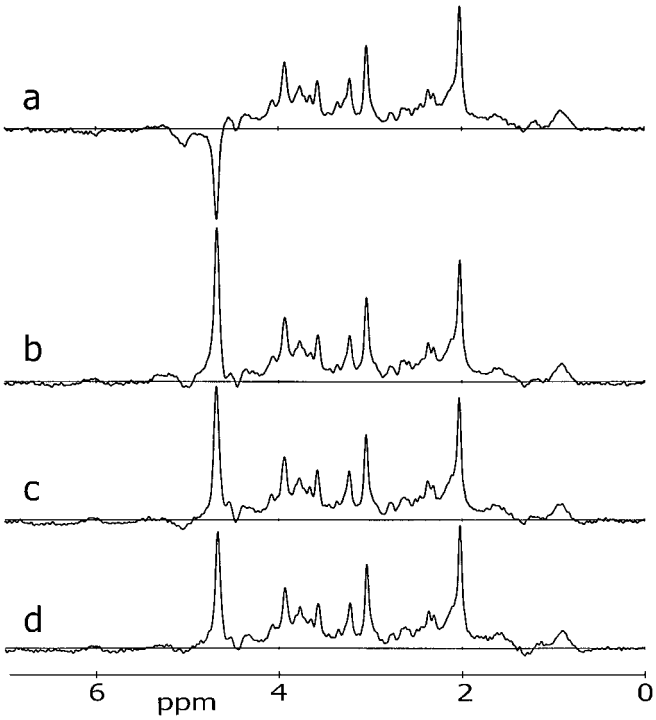

FIG. 7. ^{1}H MR spectra from a $2 \times 2 \times 2$ cm^3 VOI localized by STEAM ($TM = 50$ ms, $TE = 7$ ms) in the occipital lobe of the human brain, acquired in 256 phase-cycled scans with WS by a $3 + 1$-pulse WASHCODE sequence. The B_1 levels of 30-ms WS pulses HS -0.2 were set to (a) B_{1t}, (b) $1.4\,B_{1t}$, (c) $2\,B_{1t}$, and (d) $4\,B_{1t}$. Spectra were normalized according to the NAA peak at 2.02 ppm. Based on comparison with the NAA signal intensity, the WS factors can be estimated as 4400, 2300, 2900, and 3500, respectively. Note the high reproducibility of the metabolite part of the spectra.

sequences easy and fast to adjust and, therefore, suitable for routine clinical applications. It is worth noting that the implementation of WASHCODE sequences with simulation-based optimized parameters never required any additional adjustment to achieve a 2000- to 4000-fold suppression of the water resonance. With the long interpulse delays, lower spoiling gradients can be used in order to reduce acoustic modulation. If necessary, RF and gradient pulses for OVS can be easily incorporated into these delays without compromising the T_1 insensitivity.

The numerically optimized parameters given in Table 2 do not represent global minimizers of our objective functions. Different WASHCODE sequences tailored to specific needs may be obtained with objective functions properly reflecting the particular priorities involving various aspects of the sample investigated, field quality, and the acquisition procedure employed.

The key parameter defining the frequency profile of the suppression region is the HS-pulse length, defining the transition bandwidth. For the 3 T magnetic field, values of 30–50 ms are suitable. The suppression profile improves with increasing the number of WS pulses. Even with 4 HS pulses before the localization module, the WASHCODE sequence is usually shorter than 200–280 ms at a B_0 field of 3 T. In well-shimmed magnetic fields, the lengths of HS pulses and their frequency bandwidths can be chosen such that only the frequency range from about 4.3 to 6.0 ppm is strongly affected by the WS RF pulses.

To modify the parameters suiting the 3 T field for another B_0 field, full reoptimization may not be necessary. With simply rescaled offsets and lengths of HS pulses, identical WS performance would be guaranteed with identical delays between the apparent T_1-relaxation focus points of the HS pulses. In practice, using the same free delays and slightly adjusting the last presaturation pulse offset are often satisfactory. For instance, at B_0 of 1.5 and 7 T, durations of these sequences may be about 300–500 ms and 130–180 ms, respectively.

Finally, it may be interesting to compare the RF power deposition of WASHCODE sequences with that of other modules. Such a comparison can be based on the integral $\Xi = \int (\gamma B_1(t))^2\,dt$ if all B_1 values refer to the same point. For volume selection, the natural reference position is the center of the VOI, for which the 90° flip angle is adjusted. With high-quality selection of the VOI, only WS inside the VOI is important. For the HS pulse power adjustment, the point inside the VOI experiencing the lowest

TABLE 3
Energy Deposition by Various Localization and WS Modules (Ξ, Relative Units)

$B_{1\,max}/B_{1\,min}$	STEAM[a,g]	WET[b,g]	VAPOR[c,g]	BISTRO[d,h] (32-pulse)	SWAMP[e,h] (4-pulse)	WASHCODE[f,h,i] (4-pulse, 1-sided)
1.5	530	80	190	110	1200	190
3	530	—	—	280	3100	480

[a] 2.1-ms AM pulses P10, bandwidth 2500 Hz. For 2.1-ms 3-lobe sinc pulses: 13% less.
[b] 8.2-ms gaussian pulses, bandwidth 200 Hz. For 26.2-ms AM pulses P10: 4% more. Refs. *5–7*.
[c] 26.2-ms AM pulses P10, bandwidth 200 Hz. For 8.2-ms gaussian pulses: 4% less. Ref. *9*.
[d] 100-ms pulses HS 1.0, bandwidth 200 Hz, threshold q_e assured by the highest pulse. Ref. *13*.
[e] 30-ms pulses HS 1.0, bandwidth 667 Hz, threshold q_t. Ref. *14*.
[f] 30-ms pulses HS 0.2, bandwidth 133 Hz, threshold q_t.
[g] B_1 level set for the VOI center.
[h] For the two B_1 ranges, B_1 level in the VOI center set 25% and 100% above the threshold level.
[i] Identical for SWAMP modified for single-sided spectra, with pulses according to note (*f*) above.

RF sensitivity is decisive, i.e., the power level will be higher in the VOI center. In this sense the power deposition by the WS pulses depends on the B_1 range ($B_{1\,\min}$ to $B_{1\,\max}$) inside the VOI. For $B_{1\,\max}/B_{1\,\min}$ equal to 1.5 and 3.0 and with other reasonable assumptions, the relative amounts of energy deposited by various sequence modules are summarized in Table 3, whose values are based on data in Table 1. For simplicity, a B_1 value of $(B_{1\,\min} + B_{1\,\max})/2$ has been assumed in the VOI center. With $B_{1\,\max}/B_{1\,\min} \sim 3$, representing the practical B_1 inhomogeneity limit for STEAM localization, only WS-schemes like BISTRO (*13*), SWAMP (*14*), or WASHCODE (*15*) are useful. The differences in energy deposition, however, are substantial: for example, SWAMP (or 2-sided WASHCODE) dissipates ~6.5-times more energy than a 4-pulse 1-sided WASHCODE sequence. If required, the WASHCODE power deposition can be further decreased by reducing the number of HS pulses to 3 or 2.

CONCLUSIONS

The WASHCODE schemes systematically introduced in this paper may represent a substantial improvement for water suppression in *in vivo* proton MR spectroscopy. WASHCODE sequences are capable of providing excellent water-suppression factors, routinely exceeding 2500 and with a potential to exceed 10,000 even at very large inhomogeneities of the excitation B_1 field and of the water T_1-relaxation time, where other commonly employed WS sequences have been found considerably less successful. The proposed WASHCODE sequences are characterized by minimized RF power requirements and very small adverse effects on the spectral ranges of interest. They exhibit high flexibility and robustness. Their implementation is easy and by no means time consuming. Elimination of adjustment problems, reducing the time required to obtain spectroscopic data, together with the generally exceptional performance, makes WASHCODE sequences potentially suitable for clinical examinations.

TABLE 4
Hyperbolic-Secant Pulse Parametrizations

This work	F	n	q	λ	T
Ref. *14*	$\Delta\omega_{\max}$	$\frac{\Delta\omega_{\max} T}{2\beta}$	$\frac{\gamma B_{1\,\max}}{\Delta\omega_{\max}}$	2β	T
Ref. *21*	$-\frac{A}{\tanh\beta}$	$-\frac{A}{\beta\tanh\beta}$	$\frac{\gamma B_1^0}{A}\tanh\beta$	βT_p	T_p
Ref. *22*[a]	$\frac{\lambda}{2\pi}$	$\frac{\lambda}{2\pi\beta}$	$\frac{\omega_{1(\max)}}{\lambda}$	$2\beta\tau$	2τ
Ref. *17*	$\frac{\beta\mu}{2\pi}$	$\frac{\mu}{2\pi}$	$\frac{\Omega_0}{\beta\mu}$	βT	T
Ref. *23*	$\frac{sw}{4\pi}$	$\frac{sw}{4\pi\beta}$	$\frac{2x_f}{sw}$	βT	T
Ref. *24*	$\Delta\nu_{\max}$	N	ν	Q	T_p

[a] $Q_0 = 2\pi nq^2$.

APPENDIX

The parametrization of HS pulses used in this paper has been selected with regard to the simplicity of formulating general statements relevant to the topics studied. Table 4 gives an overview of the relations of these parameters to several other mathematically equivalent parametrizations found in literature (*14, 17, 21–24*).

ACKNOWLEDGMENTS

This work was supported by the Academy of Sciences of the Czech Republic (Grant A4065901), by a project of Czech-Austrian cooperation KONTAKT (Grant 2000/9), and by Jubiläumsfonds of the Österreichische Nationalbank (Grant 7987). V.M. and E.M. acknowledge additional support by the LBI Experimental and Clinical Radiology. Z.S. Jr. is grateful to Jana Starčuková for her software support of off-site data processing.

REFERENCES

1. R. E. Hurd, D. Gurr, and N. Sailasuta, Proton spectroscopy without water suppression: The oversampled J-resolved experiment, *Magn. Reson. Med.* **40,** 343–347 (1998).
2. A. Haase, J. Frahm, W. Hänicke, and D. Matthaei, ^{1}H proton NMR chemical shift selective (CHESS) imaging, *Phys. Med. Biol.* **30,** 341–344 (1985).
3. C. T. W. Moonen and P. C. M. van Zijl, Highly effective water suppression for in vivo proton NMR spectroscopy (DRYSTEAM), *J. Magn. Reson.* **88,** 28–41 (1990).
4. J. F. Shen and J. K. Saunders, Double inversion recovery improves water suppression in vivo, *Magn. Reson. Med.* **29,** 540–542 (1993).
5. R. J. Ogg, P. B. Kingsley, and J. S. Taylor, WET, a T_1- and B_1-insensitive water-suppression method for in vivo localized ^{1}H NMR spectroscopy, *J. Magn. Reson. B* **104,** 1–10 (1994).
6. T. Ernst and J. Hennig, Improved water suppression for localized in vivo ^{1}H spectroscopy, *J. Magn. Reson. B* **106,** 181–186 (1995).
7. S. H. Smallcombe, S. L. Patt, and P. A. Keifer, WET solvent suppression and its application to LC NMR and high-resolution NMR spectroscopy, *J. Magn. Reson. A* **117,** 295–303 (1995).
8. Z. Starčuk Jr., I. Tkáč, and Z. Starčuk, Localized proton MR spectroscopy: Short echo-time STEAM sequence with a new approach to T_1 insensitive highly effective water suppression, Proceedings of the International Society of Magnetic Resonance in Medicine, 5th Annual Meeting, Vancouver, p. 1459, 1997.
9. I. Tkáč, Z. Starčuk, I.-Y. Choi, and R. Gruetter, in vivo ^{1}H NMR spectroscopy of rat brain at 1 ms echo time, *Magn. Reson. Med.* **41,** 649–656 (1999).
10. B. D. Ross, H. Merkle, K. Hendrich, R. S. Staewen, and M. Garwood, Spatially localized in vivo ^{1}H magnetic resonance spectroscopy of an intracerebral rat glioma, *Magn. Reson. Med.* **23,** 96–108 (1992).
11. B. A. Inglis, K. D. Sales, and S. C. R. Williams, BIRIANI: A new composite adiabatic pulse for water-suppressed proton NMR spectroscopy, *J. Magn. Reson.* **105,** 61–64 (1994).
12. R. A. de Graaf, Y. Luo, M. Terpstra, H. Merkle, and M. Garwood, A new localization method using an adiabatic pulse, BIR-4, *J. Magn. Reson. B* **106,** 245–252 (1995).
13. R. A. de Graaf, Y. Luo, M. Garwood, and K. Nicolay, B_1-insensitive, single-shot localization and water suppression, *J. Magn. Reson. B* **113,** 35–45 (1996).

14. R. A. de Graaf and K. Nicolay, Adiabatic water suppression using frequency selective excitation, *Magn. Reson. Med.* **40,** 690–696 (1996).

15. V. Mlynárik, S. Gruber, Z. Starčuk, Z. Starčuk, Jr., and E. Moser, Very short echo time proton MR spectroscopy of human brain with a standard transmit-receive surface coil, *Magn. Reson. Med.* **44,** 964–967 (2000).

16. J. Frahm, K.-D. Merboldt, and W. Hänicke, Localized proton spectroscopy using stimulated echoes, *J. Magn. Reson.* **72,** 502–508 (1987).

17. M. S. Silver, R. I. Joseph, and D. I. Hoult, Selective spin inversion in nuclear magnetic resonance and coherent optics through an exact solution of the Bloch-Ricatti equation, *Phys. Rev. A* **31,** 2753–2755 (1985).

18. Z. Starčuk, Jr. and Z. Starčuk, Optimized asymmetric slice selective 90° and 180° RF pulses for localized MR spectroscopy, Proceedings of the Society of Magnetic Resonance, 2nd Annual Meeting, San Francisco, p. 1137, 1994.

19. D. I. Hoult, The NMR receiver: A description and analysis of design, *Prog. NMR Spectrosc.* **12,** 41–77 (1978).

20. V. Mlynárik, S. Gruber, and E. Moser, Proton T_1 and T_2 relaxation times of human brain metabolites at 3 Tesla, *NMR Biomed.* (2001), in press.

21. A. Tannús and M. Garwood, Adiabatic pulses, *NMR Biomed.* **10,** 423–434 (1997).

22. E. Kupče and R. Freeman, Stretched adiabatic pulses for broadband spin inversion, *J. Magn. Reson. A* **117,** 246–256 (1995).

23. D. Rosenfeld, S. L. Panfil, and Y. Zur, Optimization of adiabatic selective pulses, *J. Magn. Reson.* **126,** 221–228 (1997).

24. Z. Starčuk, Jr., K. Bartušek, and Z. Starčuk, Heteronuclear broadband spin-flip decoupling with adiabatic pulses, *J. Magn. Reson. A* **107,** 24–31 (1994).